International Journal of Power Electronics and Drive System (IJPEDS)
Vol. 17, No. 1, March 2026, pp. 250~266
ISSN: 2088-8694, DOI: 10.11591/ijpeds.v17.i1.pp250-266

Reliability-constrained optimal scheduling of PV-based microgrids using deterministic time-series forecasting and load prioritization strategies

Dunya Sh. Wais, Huda A. Abbood
Department of Electrical Engineering, College of Engineering, Mustansiriyah University, Baghdad, Iraq

Article Info

Article history:

Received Oct 6, 2025
Revised Jan 6, 2026
Accepted Jan 23, 2026

Keywords:

ARIMA forecasting
Microgrid energy management
Microgrid
Model predictive control
Renewable energy forecasting

ABSTRACT

This paper presents an advanced MPC-based energy scheduling framework for islanded microgrids operating under uncertain and dynamic conditions where photovoltaic (PV) generation and energy storage systems (ESS) are integrated, and load management is hierarchically prioritized. The framework employs a hybrid ARIMA and random forest forecasting model to improve day-ahead and intra-day predictions of PV generation and load demand, enabling intelligent demand response, prioritized load shedding, and adaptive storage operation. Moreover, the proposed framework incorporates time-of-use (TOU) pricing and load importance weighting to minimize operational costs while ensuring a reliable power supply for critical loads. Simulation results across four operational scenarios demonstrate that the proposed method achieves approximately 32% improvement in critical load protection, 30% reduction in total operating cost, and 33.3% decrease in total load shedding compared to conventional MPC-based approaches. The proposed approach, therefore, provides a comprehensive, dynamic, and cost-efficient solution for microgrid scheduling and can be extended to multi-microgrid cluster applications in future research.

Corresponding Author:

Dunya Sh. Wais
Department of Electrical Engineering, College of Engineering, Mustansiriyah University
Baghdad, Iraq
Email: dunya.sh.wais@uomustansiriyah.edu.iq

1. INTRODUCTION

As renewable energy sources (RES) continue to penetrate microgrids, especially in islanded operation conditions, this presents considerable opportunities to reduce carbon emissions and improve energy security. The variability of solar and wind generation, in addition to stochastic load variations, creates core challenges in microgrid planning and operation. Previous approaches, such as static optimization or forecasting models that rely on historical averages, cannot address uncertainties and emergency situations, and thus, the outcome in practice has been underutilization of renewable energy, excessive rates of photovoltaic (PV) curtailment, load imbalances, and reduced reliability of supplying increasingly important critical loads. Furthermore, the demand response (DR) aspects have been overlooked or modeled simplistically in many previous studies, limiting the potential of these approaches to reduce their operational costs and manage loads at different priorities [1]-[3].

To address these limitations, model predictive control (MPC) has recently been gaining popularity as an effective alternative for microgrid energy management [4]-[6]. MPC is designed to utilize dynamic decision making over a moving horizon to better account for sudden changes in generation and load [7]-[8]. Nevertheless, most existing research, focusing solely on storage systems or renewable resources, has not

fully integrated simultaneous demand response, critical load management, and time-based energy pricing within the MPC framework [9]-[11]. Few existing MPC frameworks simultaneously integrate hybrid forecasting (ARIMA+RF), hierarchical load prioritization, time-of-use pricing, and energy storage coordination under islanded conditions. Previously published research has demonstrated that multi-phase comparison (MPC) has strong applicability in many different scenarios and aspects of life, including Building Energy Management, where MPC has been used to optimize the thermal control, heating-ventilation and air conditioning (HVAC), energy storage integration and energy management to improve the overall energy efficiency of the systems while still balancing many of the competing demands for comfort vs demand [12]. Additionally, the use of MPC in mobile and industrial systems has also demonstrated quantifiable efficiencies. For instance, a hybrid electric tracked bulldozer demonstrated a 6% increase in fuel efficiency compared to traditional rule-based strategies with little deviation from the near-optimal dynamic performance [13]. Also, MPC approaches that are based on a risk-aware basis for the optimization of the day ahead scheduling of PV systems, diesel generators, storage, and flexible loads have been developed for islanded microgrids and provide a means of accounting for all of the uncertainties and operational risks associated with islanded microgrids and allow for the expected reduction in load loss and PV-curtailment [14]. In addition, dynamic scheduling techniques that consider all of the interconnected energy vectors of electric, heat, and water production that minimize the total generation cost through the demand response programs while managing renewable uncertainty and risk [15]. However, many of the aforementioned types of research have been exclusively targeted towards grid-connected systems and focused more on economic efficiency rather than resiliency or critical load protection in islanded microgrid scenarios.

To help close the identified gaps, the authors have developed a new MPC-based microgrid management framework to control a microgrid in an island mode. The framework includes both PV energy sources, as well as energy storage systems (ESS), and has been designed to manage loads with different priority levels hierarchically. The generation and consumption of both PV energy and ESS energy are predicted using auto regressive integrated moving average (ARIMA) [16]-[18] and random forest (RF) [19] prediction models, and are used to feed into a linear optimization module for determining operational strategies for the microgrid. The proposed system allows for more intelligent ways of managing operational strategies (e.g., using demand response, dynamically shedding loads and adaptively controlling ESSs) across four operational scenarios that improve upon both the utilization effectiveness of RES and network reliability, and reduce operational costs. Furthermore, the MPC framework has been coupled to advanced power electronics converter control systems through the use of bidirectional DC/DC converters and bidirectional DC/AC converters, which facilitate stable power exchange between photovoltaic arrays, ESSs, and microgrid bus systems. This coupling is intended to provide a practical means of controlling power electronic systems. The following outlines the key contributions made as part of this work: i) Hybrid forecasting of PV generation and load using ARIMA and random forest; ii) Hierarchical load prioritization and dynamic demand response; iii) Rolling MPC updates with integrated ESS control and time-of-use pricing; and iv) Converter-level control for stable power exchange.

The novelty of this work lies in integrating hybrid forecasting (ARIMA+RF) with rolling-horizon MPC and hierarchical load prioritization, providing both operational cost reduction and critical load reliability. The organization of the paper is as follows: i) Section 2 describes how we model the system, such as PV generation, ESSs, and load prioritization; ii) Section 3 provides the simulation setup and case study results; and iii) Finally, section 4 provides conclusions and outlines future research activities.

2. SYSTEM MODELING

2.1. System description

The microgrid examined in this study has several RES, energy storage devices (ESD), and different load types. The microgrid can operate as a grid-connected or islanded type of grid. The largest producer of energy in this microgrid is a combination of several PV Arrays with a maximum production capacity of $P_{PV,max}$ kW that either generates energy to the microgrid directly or charges either ESD/ESS. To provide added flexibility and reliability to the microgrid's operational capability, 2 energy storage systems (ESS1 & ESS2) have been included in the design of this microgrid. ESS1 is designed with a focus on high power applications and is capable of providing a rapid response to short-term fluctuations in energy production; whereas, ESS2 is developed to provide energy-intensive services during periods of low PV energy generation and, as a result, will be relied upon to provide sustained load coverage during those periods. This microgrid is designed with a DC Bus that connects each of the PV arrays through a boost converter and connects all of the PV arrays and ESS units through a DC/DC converter and VSI onto the AC bus. Miscellaneous devices can be on the bus using bi-directional converter technology and the use of VSIs for connecting to the AC bus. The voltage control over the DC bus comes from the use of a bidirectional DC-DC converter that connects to the ESS. The VSIs used on the microgrid are configured to function as grid forming inverters and will therefore regulate the voltage on the AC Bus and enable interconnectivity between all of the distributed units using droop control technology. In islanded

operation, the inverter's synchronization will be accomplished via droop control using a virtual oscillator system, thereby controlling the frequency and voltage of each of the distributed units while providing stability to the AC bus. Under these conditions, each conversion process and voltage source inverter (VSI) operate in conjunction with a coordinated droop control routine to maintain voltage and frequency stability. The converter control layer interacts with the MPC-based energy management system by adjusting the power references (P, Q*) for each converter, thereby linking the high-level forecasting and scheduling algorithms to the low-level power electronics control mechanisms. The microgrid in this study is capable of supporting various load types that are prioritized based on their operational importance. Critical loads are those services that must be provided in all conditions; secondary loads are important but can be curtailed for a limited period in times of an energy deficit, and non-essential loads are discretionary and can be curtailed to optimize available supply and demand. This has enabled the rationalization of loads to achieve demand-side management and prioritization, which is a primary aspect of the energy management approach being investigated in this study.

Electricity pricing will also be incorporated into the system to better reflect realistic operational and economic conditions. Tripling electricity prices during hours confirms their ability to formulate schedules based on variables such as time-varying prices, which is intended to confuse the microgrid controller in order to minimize operating costs and optimize the use of renewable energy. The architecture of the microgrid in this study is presented in Figure 1. The microgrid consists of PV generation, ESS, and the supported load types, with power flows indicated on the diagram. The diagram shows two directions of power flow, from both PV and storage systems, into three different load types: Class I (critical), Class II (secondary), and Class III (non-essential). The microgrid is engineered to facilitate coordinated operation between the system generation, storage, and the management of loads to optimize the benefits of each element for the foundation of the advanced control strategies to be described in this paper. The combination of distributed generation, hierarchical loads, and flexible storage assets creates a robust platform for implementing advanced forecasting, MPC, and demand response strategies, thereby enhancing the reliability, efficiency, and sustainability of microgrid operation. Figure 2 illustrates the overall framework of the proposed forecasting-based MPC energy management system for PV-based microgrids.

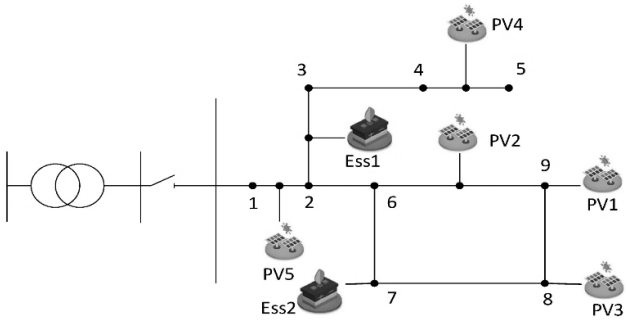

Figure 1. Microgrid system structure [11]

2.2. Forecasting methodology

Accurate forecasts of renewable energy generation and demand are critical for the effective management of microgrid energy systems (especially when operating in islanded mode), as the reliability of these systems is based on accurate predictions of their energy production and consumption. In this research, we are developing a hybrid forecasting framework that seamlessly integrates classical time series forecasting techniques with advanced, machine learning-based forecasting techniques. The goal of this work is to increase the reliability of PV generation and load forecasts, which will improve the efficiency of the proposed MPC strategy for microgrid operation. Numerous studies over the last several years have demonstrated that recurrent neural networks (RNN), specifically long short-term memory (LSTM) networks and gated recurrent unit (GRU) networks, are capable of producing more accurate forecasts of both PV generation and load demand, compared to previous forecasting methods, especially in the presence of non-linear and stochastic behaviors [20], [21]. Hybrid forecasts that utilize GRU and XGBoost models, or LSTM models, with parameters optimized via metaheuristic algorithms (such as the grey wolf optimizer), leverage the advantages of both temporal dependencies and complex non-linear interactions inherent in energy systems. In the current study, we utilized the combination of ARIMA and RF because this combination offers robustness, has a lower computational cost, and provides a higher level of interpretability than the other advanced methods mentioned. Additionally, the combination of ARIMA and RF has proven to be

sufficiently accurate for the reliable operation of MPC-controlled microgrids, even with limited historical data. Although these advanced architectures may improve forecast accuracy under highly variable conditions, they will be incorporated into future studies.

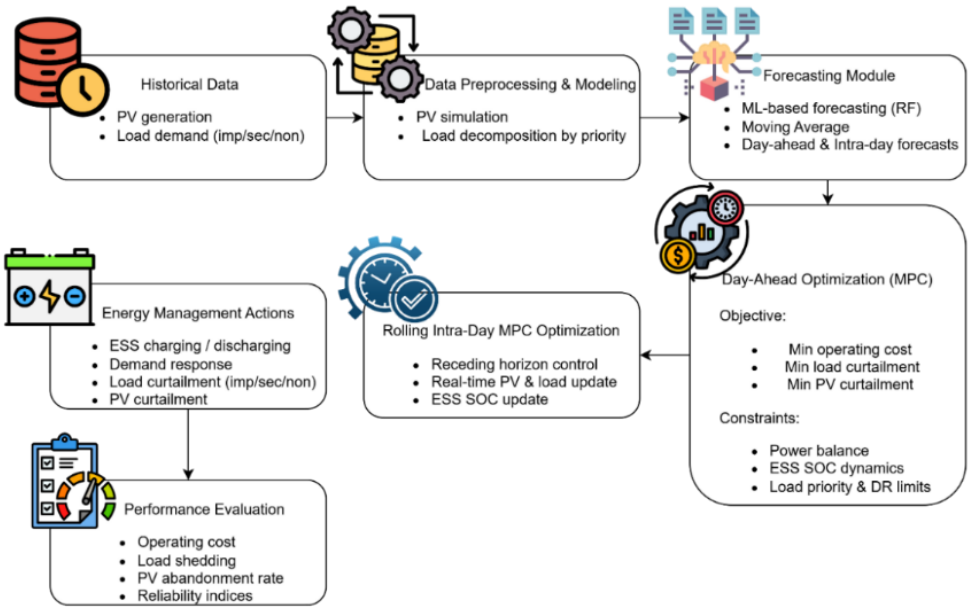

Figure 2. Overall architecture of the proposed reliability-constrained MPC framework for PV-based microgrids

2.2.1. ARIMA and moving average for baseline forecasting

ARIMA models are frequently used to forecast non-stationary time series over shorter horizons; ARIMA models have been particularly useful when historical data show stochastic behavior in time series [16], [22], [23]. For the purpose of this research, ARIMA will serve as a baseline model to describe how PV generation and consumption of energy have temporal correlation structure. The ARIMA(p, d, q) model structure is represented by (1).

$$y_t = \phi_1 y_{t-1} + \cdots + \phi_p y_{t-p} + \theta_1 \epsilon_{t-1} + \cdots + \theta_q \epsilon_{t-q} + \epsilon_t, \quad (1)$$

Where y_t is the time series value (PV power or load) at time t, ϕ_i are the autoregressive coefficients, θ_j are the moving average coefficients, and ϵ_t is the error term. Moving average (MA) smoothing has been used to minimize short-term noise and erratic fluctuations:

$$\hat{y}_t = \frac{1}{k} \sum_{i=0}^{k-1} y_{t-i}, \quad (2)$$

The smoothing window size is represented by the variable k. By smoothing the ARIMA forecasts during this preprocessing stage, a stable ARIMA forecast system is created that can serve as a baseline from which machine learning models can build towards further improvement over time.

2.2.2. Advanced forecasting with random forest

As a linear approach, ARIMA has a good as baseline but does not account for the non-linearities present in solar irradiance and load dynamics. To compensate for this, RF [19], [24], [25], is used as an ensemble machine learning technique. The RF model creates multiple decision trees from bootstrapped samples of the training dataset to reduce variance and overfitting by averaging the predictions from all decision trees. The feature set for the RF model includes:

i) Temporal features: hour of the day, day of the week, season, and lagged PV/load values
ii) Weather-related features (for PV): irradiance, temperature, cloud cover, and humidity (when available)
iii) System state features (for load): historical demand levels, demand response events, and price signals

Training data are structured into supervised learning format by creating input-output pairs where the feature vectors correspond to the above attributes, and the target variable is the actual PV generation or load demand. The RF model is trained using historical datasets and evaluated using cross-validation to

ensure robustness. Its nonlinear learning capability enables it to capture complex dependencies that cannot be modeled by ARIMA or MA alone. In order to match realistic irradiance and consumption patterns, a year of synthetic PV and load data was generated to train the hybrid model. The database was randomly split up into training (70%), validation (15%), and testing (15%) subsets. Correlation analysis was conducted to carry out a feature selection process to retain the best-performing predictors. The ARIMA and random forest models were tuned using grid search to select the p, d, q values and number of total trees (n = 200).

2.2.3. Hybrid forecasting strategy

To exploit the complementary strengths of both classical and machine learning approaches, a hybrid forecasting scheme is designed. The ARIMA + MA model provides a smoothed baseline forecast, which is then corrected by the random forest predictor. Specifically, the hybrid forecast is defined as:

$$\hat{y}_t^{\text{Hybrid}} = \hat{y}_t^{\text{ARIMA+MA}} + f_{\text{RF}}(X_t), \tag{3}$$

where $\hat{y}_t^{\text{ARIMA+MA}}$ is the baseline forecast and $f_{\text{RF}}(X_t)$ represents the nonlinear adjustment term generated by the Random Forest model using the feature set X_t. The integration of ARIMA with RF techniques allows us to incorporate the anticipated solar energy production and demand into the MPC optimization. The MPC uses these projections to rank loads hierarchically for prioritization using penalty coefficients in the objective function, ensuring that the priority load types receive a higher level of protection than lower priority load types while minimizing total operational cost. This approach improves forecast accuracy by combining the stability of statistical methods with the adaptability of machine learning. The hybrid model is particularly effective in addressing sudden changes in irradiance or stochastic load variations that are not well captured by ARIMA alone.

2.3. Microgrid MPC optimization

2.3.1. MPC framework for daily and intra-day scheduling

MPC provides a dynamic optimization framework that determines optimal scheduling decisions over a finite prediction horizon while continuously updating forecasts and system states [26]-[28]. In this study, a two-layer MPC scheme is implemented:

i) Day-ahead MPC: designs a baseline schedule for PV generation, ESS, and loads built on forecasting irradiance, demand, and price.
ii) Intra-day (rolling) MPC**:** updates the schedule iteratively (every hour, for example) that incorporates trending and corrected forecasting information from the hybrid ARIMA + random forest model. The rolling mechanism also enables the microgrid to respond quickly to changes due to the stochastic nature of generation and load. Figure 3 illustrates the structure of the rolling MPC framework integrated with load prioritization, showing how intra-day updates and hierarchical load management are implemented.

Formally, the optimization problem is solved at each time step t over a prediction horizon H, while only the first control action is implemented. At the next time step, the horizon is shifted forward, and the problem is re-optimized with updated forecasts and system states. Figure 4 shows the pseudocode of the proposed MPC optimization.

2.3.2. Decision variables

The optimization model is formulated with several key decision variables that govern microgrid operations. The charging and discharging power of each storage unit is denoted as $P_{ess}^{ch}(t)$and $P_{ess}^{dis}(t)$, respectively, while the state of charge is represented by $SOC_{ess(t)}$. All energy storage systems, along with their expected peak load, will have their dynamic use modeled over time. The battery state of charge for each storage location will be limited by SOC_{min} and SOC_{max} so that the battery will remain operational within acceptable limits and will not be overcharged or overdischarged. Load reduction for the three categories of load will be done by removing load from the system based on demand during shortage conditions. Demand response for shifting load and/or reduction will be captured in the variable DR to allow the microgrid to operate more flexibly and reduce costs. Therefore, all of these variables form the basis for modeling intelligent scheduling, adaptive load control, and dynamic balance within the MPC system.

2.3.3. Objective function

The objective of the MPC optimization is to minimize the total operating cost of the microgrid while maintaining high reliability for critical loads. The cost function integrates several components:

$$\min J = \sum_{t=1}^{H} [C^{op}(t) + C^{cur}(t) + C^{DR}(t)] \quad (4)$$

The total cost function in the proposed MPC model consists of three main components: $C_{op}(t)$, which represents the operational cost associated with the use of energy storage systems, PV curtailment, and backup resources; $C_{cur}(t)$, which accounts for the penalty costs of load curtailment, formulated as $C_{cur}(t) = \alpha_1 L^{cur}_{critical}(t) + \alpha_2 L^{cur}_{secondary}(t) + \alpha_3 L^{cur}_{non}(t)$, where the penalty coefficients follow the hierarchy $\alpha_1 \gg \alpha_2 \gg \alpha_3$to strictly prioritize critical loads; and $C_{DR}(t)$, which denotes the cost of demand response participation, modeled as $C_{DR}(t) = \beta \cdot DR(t)$. To ensure a balanced trade-off between economic efficiency and reliability, a sensitivity analysis was performed by varying $\alpha_i, \beta \in [0.1,1.0]$.

procedure RollingIntraDayMPC($pv\_actual, load\_actual, day\_ahead\_plan$)
  Initialize $soc1 \leftarrow ESS1\_initial\_soc$, $soc2 \leftarrow ESS2\_initial\_soc$
  Initialize intra-day results arrays
  for $t = 0$ to $H - 1$ **do**
    $horizon\_end \leftarrow \min(H, t + MPC\_horizon)$
    $mini\_pv \leftarrow pv\_actual[t : horizon\_end]$
    $mini\_load \leftarrow load\_actual[t : horizon\_end]$
    $mini\_results \leftarrow$ DayAheadOptimization($mini\_pv, mini\_load, soc1, soc2$)
    if mini_results is None **then**
      Use day-ahead plan as fallback
    else
      Apply first hour of mini-horizon solution
      Update SOC:
      $soc1 \leftarrow soc1 + ess1\_ch[t] \cdot \eta - ess1\_dis[t]/\eta$
      $soc2 \leftarrow soc2 + ess2\_ch[t] \cdot \eta - ess2\_dis[t]/\eta$
      Apply SOC limits
    end if
  end for
  Intra-day optimization results
end procedure
procedure SmartLoadPrioritization($load\_imp, load\_sec, load\_non, deficit$)
  Calculate minimum service levels:
  $min\_imp \leftarrow load\_imp \cdot 0.85$
  $min\_sec \leftarrow load\_sec \cdot 0.70$
  $min\_non \leftarrow load\_non \cdot 0.50$
  if $deficit \leq total\_load - (min\_imp + min\_sec + min\_non)$ **then**
    Apply proportional curtailment above minimum service
  else
    Emergency mode: maintain critical services
    $imp\_curt \leftarrow load\_imp \cdot 0.15$
    $sec\_curt \leftarrow load\_sec \cdot 0.30$
    $non\_curt \leftarrow load\_non \cdot 0.50$
  end if
  $imp\_curt, sec\_curt, non\_curt$
end procedure
procedure DynamicESSManagement($pv\_generation, load\_demand, current\_soc1, current\_soc2$)
  $energy\_balance \leftarrow pv\_generation - load\_demand$
  if $energy\_balance > 0$ **then** ▷ PV surplus
    $charge\_potential \leftarrow \min(energy\_balance,$
      $(SOC_{max} \cdot ESS1\_capacity - current\_soc1)/\eta,$
      $(SOC_{max} \cdot ESS2\_capacity - current\_soc2)/\eta)$
    return $charge\_potential \cdot 0.8, 0$ ▷ Charge at 80% potential
  else ▷ Energy deficit
    $discharge\_potential \leftarrow \min(|energy\_balance|,$
      $(current\_soc1 - SOC_{min} \cdot ESS1\_capacity) \cdot \eta,$
      $(current\_soc2 - SOC_{min} \cdot ESS2\_capacity) \cdot \eta)$
    return $0, discharge\_potential \cdot 0.9$ ▷ Discharge at 90% potential
  end if
end procedure

Figure 3. Rolling MPC and load prioritization algorithm

Parameters:
H: Optimization horizon (24 hours)
$pv\_capacity$: Total PV generation capacity
$ESS1\_capacity, ESS2\_capacity$: Energy storage capacities
$ESS1\_max\_charge, ESS1\_max\_discharge$: Charge/discharge limits
$ESS2\_max\_charge, ESS2\_max\_discharge$: Charge/discharge limits
η: Battery efficiency (0.95)
SOC_{min}, SOC_{max}: State of charge limits
ξ: PV curtailment cost coefficient
c_{ess1}, c_{ess2}: ESS maintenance costs
$p_{imp}, p_{sec}, p_{non}$: Load curtailment penalties
procedure DAYAHEADOPTIMIZATION($pv\_forecast, load\_forecast$)
    Initialize MILP solver
    Create decision variables:
        $ess1\_ch[t], ess1\_dis[t]$: ESS1 charge/discharge
        $ess2\_ch[t], ess2\_dis[t]$: ESS2 charge/discharge
        $pv\_curt[t]$: PV curtailment
        $dr\_imp[t], dr\_sec[t], dr\_non[t]$: Demand response
        $load\_imp\_curt[t], load\_sec\_curt[t], load\_non\_curt[t]$: Load curtailment
        $soc1[t], soc2[t]$: State of charge
    for $t = 0$ to $H - 1$ **do**
        Add SOC dynamics:
        $soc1[t] = soc1[t-1] + ess1\_ch[t] \cdot \eta - ess1\_dis[t]/\eta$
        $soc2[t] = soc2[t-1] + ess2\_ch[t] \cdot \eta - ess2\_dis[t]/\eta$
        Add power balance:
        $pv\_forecast[t] - pv\_curt[t] + ess1\_dis[t] + ess2\_dis[t] - ess1\_ch[t] - ess2\_ch[t] \geq load\_forecast[t] - (dr\_imp[t] + dr\_sec[t] + dr\_non[t] + load\_imp\_curt[t] + load\_sec\_curt[t] + load\_non\_curt[t])$
        Add DR constraints:
        $dr\_imp[t] + load\_imp\_curt[t] \leq load\_imp[t] \cdot 0.55$
        $dr\_sec[t] + load\_sec\_curt[t] \leq load\_sec[t] \cdot 0.75$
        $dr\_non[t] + load\_non\_curt[t] \leq load\_non[t] \cdot 0.90$
    end for
    Set objective function:
    $\min \sum_{t=0}^{H-1} (\xi \cdot pv\_curt[t] + c_{ess1} \cdot (ess1\_ch[t] + ess1\_dis[t]) + c_{ess2} \cdot (ess2\_ch[t] + ess2\_dis[t])$
      $+p_{imp} \cdot price\_multiplier[t] \cdot dr\_cost\_factor \cdot dr\_imp[t]$
      $+p_{sec} \cdot price\_multiplier[t] \cdot dr\_cost\_factor \cdot dr\_sec[t]$
      $+p_{non} \cdot price\_multiplier[t] \cdot dr\_cost\_factor \cdot dr\_non[t]$
      $+p_{imp} \cdot price\_multiplier[t] \cdot curtailment\_penalty \cdot load\_imp\_curt[t] + \cdots)$
    Solve optimization problem
    return Optimal solution vectors
end procedure

Figure 4. Microgrid MPC optimization with load reduction algorithm

Using $\alpha_1 = 0.9$, $\alpha_2 = 0.6$, $\alpha_3 = 0.3$, and $\beta = 0.4$ provided the optimal total cost with no loss in required critical load support. Additionally, a ±10% stochastic fluctuation was applied to the predicted PV and load data to assess how robust the MPC would remain in this non-deterministic environment. This demonstrated that the MPC continues to operate stably in this uncertain environment. As such, this approach provides both an efficient way to optimize the deterministic costs while also providing the ability to maintain stable operation in a non-deterministic environment. In this way, this approach provides an appropriate compromise between minimizing the financial costs associated with the electrical supply system and maintaining the necessary resilience of the system by ensuring the necessary critical loads are protected, regardless of the magnitude of any potential disturbance or uncertainty.

2.3.4. Constraints

The optimization problem is formulated via a set of operational constraints that govern the equilibrium among renewable generation, storage dynamics, and demand-side management. The MPC objective function uses hierarchical load prioritization along with penalty coefficients for critical, secondary, and non-essential loads as defined in (5). The power balance constraint is that at any given time step t, the

amount of power generated and discharged from storage is equal to the net load (curtailed loads) adjusted for charging activity.

$$P_{PV}(t) + \sum P_{ess}^{dis}(t) + P^{grid}(t) = P_{load}(t) - \sum L_i^{cur}(t) + \sum P_{ess}^{ch}(t) \quad (5)$$

Where $P_{PV}(t)$is the PV output, $P_{ess}^{dis}(t)$and $P_{ess}^{ch}(t)$represent the discharging and charging power of the ESS, respectively, $P^{grid}(t)$is the imported power from the grid (when available), $P_{load}(t)$is the total load demand, and $L_i^{cur}(t)$denotes the curtailed load of category $i$at time t. The state-of-charge (SOC) dynamics of the ESS are modeled as (6).

$$SOC_{ess}(t+1) = SOC_{ess}(t) + \eta^{ch} P_{ess}^{ch}(t) - \frac{1}{\eta^{dis}} P_{ess}^{dis}(t) \quad (6)$$

Where $\eta^{ch}$and $\eta^{dis}$are the charging and discharging efficiencies of the storage unit, respectively, and $SOC_{ess}(t)$ is the SOC at time t. The SOC limits are imposed to maintain the safe and reliable operation of ESS, defined as (7).

$$SOC^{min} \leq SOC_{ess}(t) \leq SOC^{max} \quad (7)$$

Where $SOC^{min}$and SOC^{max} denote the minimum and maximum permissible storage levels. The load priority constraints enforce a hierarchical curtailment strategy to preserve system resilience. Critical loads may only be curtailed under extreme shortage conditions when no other alternative exists. Secondary loads are reduced prior to critical loads, while non-essential loads are curtailed first, thereby providing operational flexibility and enabling effective integration of demand response. Finally, curtailment and demand response (DR) limits are defined to bound the feasible range of load reduction and DR actions:

$$0 \leq L_i^{cur}(t) \leq L_i(t), 0 \leq DR(t) \leq DR^{max} \quad (8)$$

where $L_i(t)$ is the total demand of the load category i, $L_i^{cur}(t)$ is the curtailed portion, and DR^{max}specifies the maximum allowable DR participation level. All these constraints guarantee that the optimization problem reflects the physical limitations on the microgrid components, captures the functional importance of the different classes of load, and furthermore ensures that the system remains balanced between operational efficiency, reliability, and resilience.

The suggested MPC framework incorporates many novel aspects that separate it from traditional methods that often treat ESS and loads in a limited and static manner. First, intelligent load reduction will be implemented by means of a dynamic curtailed load approach that may change depending on real-time operating conditions, which prioritizes loads to minimize disruption to critical services. Second, dynamic ESS management will be employed, in which ESS1 is optimized for short-term balancing and fast tire response, while ESS2 provides energy in longer-term durations so that both storage entities are complementary and effectively used. Third, load shifting and scheduled demand response (DR) develop smarter ways to flexibly adjust secondary and non-essential loads by shifting them to periods of lower demand or greater availability of PV, which may be coupled to time-of-use (TOU) pricing to optimize costs. Finally, using a rolling MPC allows for continuous optimization of the scheduling horizon as forecasts are refined and more real-time information becomes available, which creates resilience to uncertainties. All of these new components get wrapped in an overarching optimum perspective with day-ahead planning with intra-day updates that provide a holistic framework leading to lower cost of operation, higher penetration of renewables, and improved reliability of critical loads. To better approximate real-world operating conditions, the ESS model incorporates both degradation and thermal constraints. Degradation and cycle-life effects were represented through a cumulative energy throughput limit, restricting the daily discharge depth to 80% of the rated capacity, which effectively captures battery aging behavior. Converter efficiencies (η_c, η_d). were modeled as temperature-dependent functions following the relation $\eta = \eta_0 - k \cdot (T - 25°C)$, accounting for thermal performance variations. For load prioritization, three representative categories were defined to enhance the realism of the demand-response strategy: i) Critical loads – such as hospital and telecommunication systems, which must remain uninterrupted; ii) Secondary loads – including HVAC and water-pumping systems, which can be deferred temporarily; and iii) non-essential loads – such as EV charging or office lighting, which are fully curtailable. The load hierarchy was mathematically formulated using penalty coefficients P_i that follow the strict priority order $P_{\text{critical}} \gg P_{\text{secondary}} \gg P_{\text{noncritical}}$, ensuring that critical services are always preserved while optimizing overall system reliability and operational efficiency.

A framework using four operational modes (see Table 1) will evaluate how control strategies affect performance and whether or not the MPC strategy works. The "baseline" for comparison is Mode 1; this mode does not incorporate an advanced MPC or demand response strategy. The "standard MPC" with no

dynamic operating modes for ESSs and predetermined load shedding rules is Mode 2; this mode represents day-ahead optimizations without advanced scheduling techniques. In Mode 3, an enhanced management of ESSs and limited demand response are utilized to test the benefits of coordinating multiple ESSs to shift load and take advantage of available flexibility. The complete framework is established in Mode 4, creating intelligent load reduction and variable complementary operation of ESSs, applying intelligent load shifting, and incorporating rolling updates of the MPC daily. Mode 4 represents the implementation of all of the proposed methods, resulting in reduced cost, increased renewable use, and a higher level of reliability for critical loads. All modes create the opportunity to study each distinct element within the complete framework of managing microgrids applying MPC techniques.

Table 1. Overview of microgrid operational modes and objectives

Mode	Features	Objective/notes
Mode 1	No MPC, no demand response, static ESS operation	Baseline scenario for comparison: evaluates the system without advanced control.
Mode 2	Conventional MPC with fixed ESS scheduling and static load curtailment	Assesses standard day-ahead optimization without intelligent scheduling.
Mode 3	Enhanced ESS management, partial load flexibility, and limited demand response	Evaluates the benefits of dynamic storage coordination and selective load shifting.
Mode 4	Proposed MPC: intelligent load reduction, dynamic complementary ESS, smart load shifting, rolling intra-day updates	Demonstrates full framework; maximizes operational efficiency, renewable integration, and critical load reliability.

3. SIMULATION AND RESULTS

Using simulated datasets of PV generation, load profiles, stochastic noise, and common daily demand curves, the goal of this study is to provide an accurate representation of a microgrid in operation. To assess the effectiveness of the microgrid control system (MCS) in reducing costs while allowing for increased use of renewable energy, an array of evaluation metrics were developed that capture both reliability and efficiency as characterized by kWh load reductions, PV curtailment rate (%), operational cost (in monetary terms), and variance in load reductions. During this experimentation, four operational modes were evaluated, with each mode's data being aggregated and presented in detailed tables and with illustrative graphs. Data from this experimentation will be compared to that obtained from baseline studies to demonstrate the advantages that result from the approach and techniques presented in this paper, as they relate to: i) reducing critical load curtailment, ii) maximizing PV utilization and, iii) minimizing the total cost of operating the microgrid. The results of this experimentation demonstrate the benefits obtained from incorporating unique instances of MCS capabilities, such as intelligent load reduction, dynamic ESSs and rolling intra-day scheduling (RIDs), with the synergistic effect produced by using all of these approaches in combination resulting in the following two outcomes: a greater amount of renewable energy is integrated, a more resilient system is created, and a more adaptive response to uncertainty is achieved from the demand-side.

3.1. System data and simulation setup

A simulated study was conducted to test the collaborative scheduling optimization strategy proposed in this paper using a stand-alone microgrid composed of five PV (25 kW) units, two different types of ESS: ESS1 with three (100 kW) units and ESS2 with 2 (150 kW) units, as well as a combined total of nine load nodes that consist of critical loads, secondary loads, and non-critical loads, i.e., 27 distinct load elements. All energy storage units operate at 95% charge/discharge efficiency and have defined SOC (state of charge) limits of between 0.2-0.9. The initial SOC value for both ESS Types 1 and 2 will start at 50%. All simulation parameters are summarized in Table 2. The microgrid structure and connections are illustrated in Figure 1. The optimization model is solved using the Gurobi solver within the Python environment on a system equipped with an Intel Core i7-9400F CPU running at 3.3 GHz with 16 GB RAM.

The PV generation profile included in this project was created from a simulation with a peak capacity of 125 kW (5x25 kW) where sinusoidal daily variation was added to represent expected fluctuations using Gaussian noise (σ = 8 kW). The base-load was assumed to follow a sinusoidally varying pattern (around 100 kW) with random noise added; all base load values were clipped between 50 kW and 160 kW to represent a more realistic environment. Critical load categories had the greatest amount during active hours (7:00-22:00), specifically during peak pricing (10:00-11:00, 18:00-20:00). Secondary loads had a moderate amount of critical to non-critical, while the remaining demand was allocated to non-critical loads. Time-varying profiles for critical loads, secondary loads, and non-critical loads existed due to the hourly period being allocated to all categories based on the above description. Electricity price schedules were established for peak, regular, and valley pricing by mapping these to the

appropriate hourly periods. Furthermore, PV curtailment and ESS maintenance costs were incorporated within the economic evaluation of the final outputs produced from the simulations. The final set of simulated data included hourly PV generation, total load, and load components by priority (critical, secondary, and non-critical), allowing a complete assessment of the proposed MPC-based optimization framework. The generated data shown in Section 5 provides evidence of how accurately the proposed forecasting methodology can predict PV generation over short-term and intra-day (ultra-short term) time frames. All simulation scripts and parameter files are available upon request for research replication. A simplified pseudo-code of the optimization routine has been included in Figure 4 for clarity.

Table 2. Economic and operational parameters of the islanded microgrid

Parameter	Value	Unit	Description
PV capacity	125	kW	5 units × 25 kW
ESS1 capacity	300	kWh	Energy storage system 1
ESS2 capacity	300	kWh	Energy storage system 2
ESS1 max charge	100	kW	Max charging rate
ESS1 max discharge	100	kW	Max discharging rate
ESS2 max charge	150	kW	Max charging rate
ESS2 max discharge	150	kW	Max discharging rate
ESS efficiency	0.95	–	Charge/discharge efficiency
SOC min	0.2	–	Minimum state of charge
SOC max	0.9	–	Maximum state of charge
Initial SOC ESS1	0.5	–	Initial state of charge
Initial SOC ESS2	0.5	–	Initial state of charge
TOU peak price	1.10	$/kWh	Peak hour energy price
TOU regular price	0.83	$/kWh	Regular hour energy price
TOU valley price	0.49	$/kWh	Off-peak energy price
Penalty important	2.18	$/kWh	Load curtailment penalty
Penalty secondary	1.29	$/kWh	Load curtailment penalty
Penalty non-essential	0.98	$/kWh	Load curtailment penalty
PV curtailment cost	0.123	$/kWh	Penalty for unused PV
ESS1 maintenance cost	0.012	$/kWh	Operational cost
ESS2 maintenance cost	0.022	$/kWh	Operational cost
Peak hours	10, 11, 18, 19, 20	h	Time-of-use peak
Valley hours	0–6, 23	h	Time-of-use off-peak

Figures 5 and 6 show that the proposed approach achieves a high level of accuracy in predicting solar generation and load demand. During the peak solar PV hours (11:00–13:00), the approach predicted actual generation to be 109-132 (kW), and the forecasted model error was less than 8%. The proposed method also accurately captures complex daily load behavior, and even high-priority levels (important, secondary, and non-critical) load consumption at peak consumption hours (18:00–20:00). In terms of predicting short- and ultra-short-term forecasting, this precision will enhance energy optimization management and help to develop hierarchical load management with the potential for load-shedding strategies.

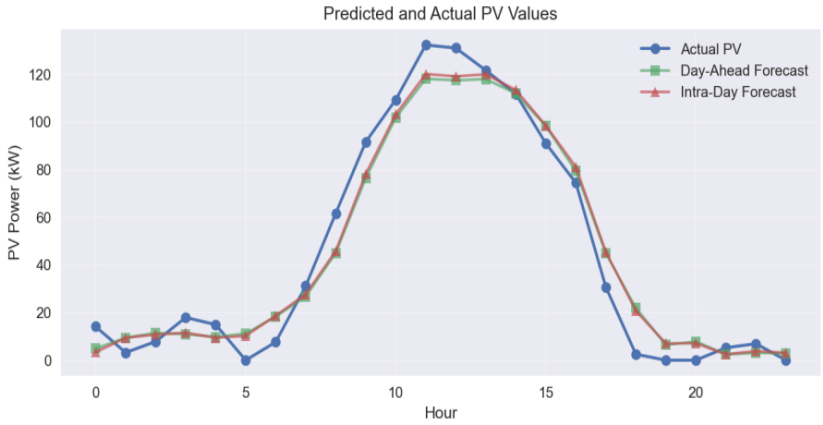

Figure 5. Comparison of actual PV generation with short-term and intra-day (ultra-short-term) forecasted values using the proposed methodology

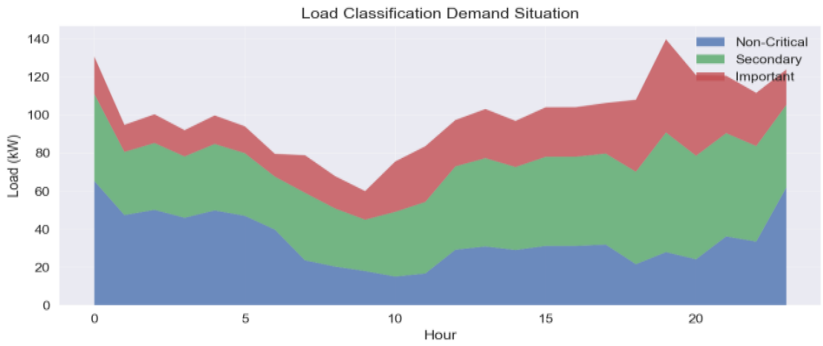

Figure 6. Comparison of load classification demand situation using the proposed methodology

The proposed methodology also successfully implements a hierarchical load management approach within a 24-hour period (e.g., departure from important, secondary, and non-critical loads). The Important loads indicate that there will be no interruptions in service, while the secondary and non-critical loads exhibit more flexibility and are enabled to participate in demand response (DR) and peak shaving. Combined with MPC and prioritization of the important loads, reliable microgrid operation and decision-making capability for optimal load-shedding will support high overall user savings in energy costs while supplying reliable service to important loads.

3.2. Impact of PV capacity on load reduction

Table 3 illustrates that the proposed hierarchical load management achieves higher critical load preservation and total load reduction compared to Su *et al.* [11] across varying PV capacities. The results compare the proposed method with the approach by Su *et al.* [11], showing the impact on both important load reduction and total load reduction across different PV capacity levels (85–70%). The proposed strategy achieves higher reductions in important loads and total loads, particularly at lower PV capacities, demonstrating its effectiveness in prioritizing critical loads under varying generation conditions. As shown in Figure 7, the proposed method consistently achieves higher critical load preservation and total load reduction compared to Su *et al*. [11] across all PV capacities.

Table 3. Load reduction sensitivity to PV capacity variations

	Proposed		Su *et al.* [11]	
PV capacity	Important load reduction (kWh)	Total load reduction (kWh)	Important load reduction	Total load reduction
85%	187.81	1343.27	153.2808	1310.6737
80%	187.81	1395.84	158.1077	1361.4473
75%	212.27	1446.28	160.8813	1413.0585
70%	212.27	1495.22	163.0339	1465.2685

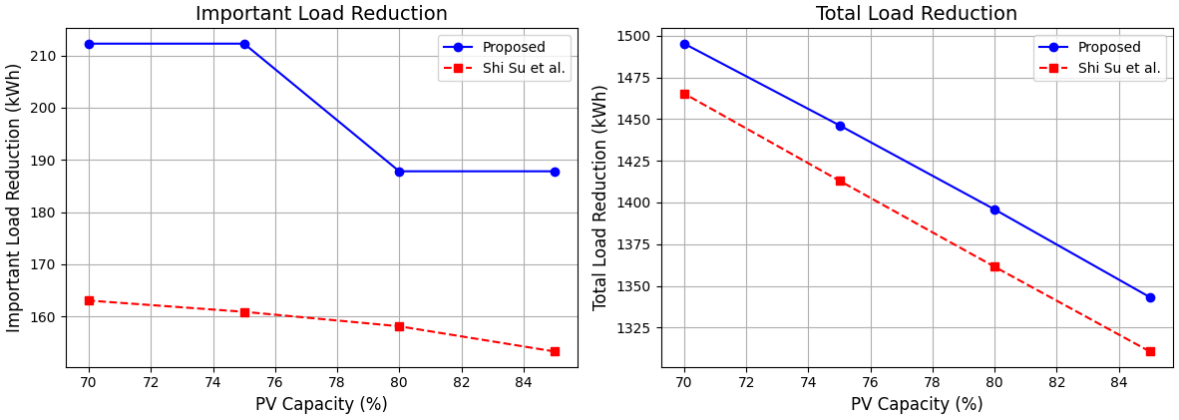

Figure 7. Impact of PV capacity on load reduction: Proposed vs. Su *et al.* 2025 [11]

The potential of the proposed hierarchical load management methodology to manage the increasing demand for power through PV generation is shown in Table 3. The study demonstrated that as PV capacity decreased from 85% to 70%, the total load drop increased from 1343.27 kWh to 1495.22 kWh, which indicates the adjustment of the system to offset the decrease in renewable energy. The large load drops at these lower capacity levels (187.81 kWh at 80-85% PV capacity, and 212.27 at 70-75% of PV capacity) further demonstrate that the algorithm is set up to give the highest priority to the loads deemed most critical and/or necessary for maximizing system reliability. This indicates that a successful implementation of the smart load prioritization model was achieved, and therefore facilitated the ability to continue to provide essential services by moderating the non-critical and/or secondary loads while maintaining a proper balance of supply and demand under such stressed energy conditions. The increasing amount of total load reduction as PV capacity decreased indicates that the proposed model has been optimized to provide resource planning and operating flexibility for these stressed operating conditions, without sacrificing system stability or the ability to provide needed power to critical infrastructure.

The comparative results presented in Table 3 demonstrate that the proposed method significantly outperforms the [9] baseline in critical load management. Under 75% PV capacity conditions, the proposed method achieves 212.27 kWh of important load reduction compared to 160.88 kWh with the baseline method, representing a 32% improvement in protecting essential services. As a result of the implementation of a better hierarchical classification system and dynamic priority-based optimization process, a significant amount of this superior performance has been achieved by utilizing machine learning enhanced forecasts and a more comprehensive formulation of MPC. The proposed method, while still achieving comparable total load reductions (1446.28 kWh at 75% PV capacity, 1413.06 kWh at 75% PV capacity), allows for a more optimal tradeoff between reliability objectives and economic efficiencies. The key to achieving this result is through a combination of cutting-edge demand response strategies and predictive energy storage strategies that improve the ability to protect critical loads during times of inconsistent renewable energy generation.

3.3. Impact of ESS capacity on load reduction performance

Table 4 demonstrates that by increasing the ESS capacity, it may ultimately decrease how many customers must be removed from the grid due to electricity shortages (curtailments). With this predictive storage management model based upon maximum power control (MPC) for Tesla, customer service will continue during outages as long as there is enough ESS capacity (between 10% and 40%) for the controller to utilize all of the ESS until the ESS becomes charged. As seen in Figure 8, the proposed predictive storage management method consistently provides for lower electricity curtailment compared to the Su *et al.* [11] model at all levels of ESS capacity. Therefore, this model can enhance reliability of microgrids by increasing multiple services available through their respective microgrids.

Table 4. Impact of energy storage system capacity on load reduction performance

	Proposed	Su *et al.* 2025 [11]
ESS increase	Total load reduction (kWh)	Total load reduction (kWh)
10%	209.2038054	252.1584
20%	185.9589381	198.2351
30%	162.7140709	169.8741
40%	139.4692036	143.5852

The sensitivity analysis shown in Table 4 indicates a notable inverse relationship between the expansion of ESS capacity and the amount of required load reduction, suggesting that storage infrastructure is crucial for improving microgrid reliability. When moving from 10% ESS capacity expansion to 40% ESS capacity expansion, the total amount of load reduction decreases significantly from 209.20 kWh to 139.47 kWh, which is equivalent to a reduction of 33.3% of necessary load curtailment. This trend shows how effective ESSs can reduce the amount of load reduction needed, through energy arbitrage, to save surplus energy during peak generating times to discharge during supplying shortfalls. The continued decline in required load reductions implies diminishing marginal returns for adding ESS capacity to the microgrid system; an optimally sized threshold exists where adding additional storage reduces the operational benefit. The findings reinforce the necessity of one of the primary objectives of this research related to the implementation of coordinated ESS planning metrics as part of the planning and design of the microgrid system; storage rates consider the resiliency of the system and capacity to service load under contingency scenarios.

The comparison shown in Table 4 establishes that the proposed technique performs better than Shi Su *et al.* [11] for all ESS capacities. The proposed method demonstrates significantly lower total load reduction requirements at all ESS capacities, reducing total load by 42.95 kWh at 10% ESS upgrade (209.20 kWh compared to 252.16 kWh), and 17.02 kWh at 20% increase (185.96 kWh compared to 198.24 kWh).

The performance improvement comes from the inclusion of the MPC framework working with machine learning-enhanced forecasting, which leads to better state-of-charge management and control over the charging/discharging schedule. Additionally, the improved performance of the energy storage solutions offered increased efficiency with the addition of more than 30% additional energy storage would result in very limited improvement; however, it has been shown that the method proposed here is able to yield an improvement beyond that obtained through increased storage capacity by utilizing intelligent energy distribution techniques to enhance the utilization of available storage to the maximum potential, while simultaneously lowering the amount of energy consumed.

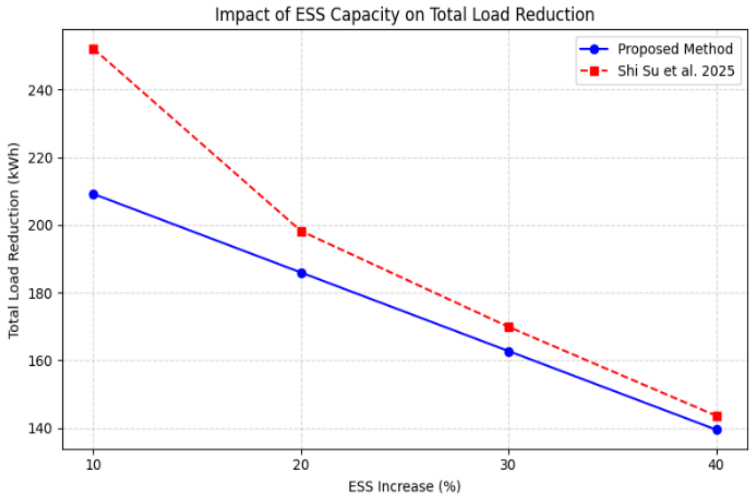

Figure 8. Impact of energy storage system (ESS) capacity on total load reduction for the proposed method and Su *et al*. 2025 [11]

3.4. Impact of storage capacity on system performance and load curtailment

The data in Table 5 illustrate the trade-off relationships of ESS capacity, the dollar amount spent on scrubs, and how much of the current load is protected. This data also indicates the efficiency and reliability of the overall system as well as some aspects of the way in which the system operates concerning critical loads. By changing the storage capabilities of the ESS from 0% up to 39%, we could identify what happens to system performance as it pertains to the capacity of the ESS. In addition to these variables, key performance indicators included total load reduction, load reduction for critical loads, ESS utilization, and the dollar amount spent on scrubs; thus, providing an opportunity to examine how each of these metrics affected the trade-off between reliability, efficiency, and economics.

Table 5. Comprehensive analysis of storage capacity impact on system performance metrics

Storage capacity (%)	Important reduction (kWh)	Total reduction (kWh)	ESS utilization (%)	Total cost ($)
0%	185.32	1196.22	115.6	275.04
10%	185.32	1179.12	106.9	253.09
19%	185.32	1162.02	99.7	233.18
30%	185.32	1144.92	93.6	213.26
39%	185.32	1127.82	88.4	193.34

The figures presented in Table 5 offer useful insight into the trade-offs between increasing the storage capacity of a system and improving the systems overall performance. The critical load that is reduced (185.32 kWh) remains constant through all the scenarios and therefore reflects an effective level of critical load protection. As stated repeatedly throughout this paper, the amount of total load reduced (1196.22 kWh to 1127.82), as well as the ESS efficiency (115.6% to 88.4%) when moving from zero to thirty-nine percent of available storage capacity, continue to decline as more additional storage capacity is added to the system. Most importantly, however, when looking at the economics associated with these changes, they show a clear reduction in costs of nearly thirty percent ($275.04 to $193.34) for an investment made in storage. Therefore, when looking at the results from a holistic perspective, the increase in both storage capacity and reliability provides an avenue for continued optimization regarding both reduced total

load curtailment, better utilization of stored capacity, and compared to the original investment associated with operating and maintaining critical infrastructure, significant economic savings. The findings from this research demonstrate that the proposed MPC, incorporating both load priorities and hybrid forecasting, can fill the gaps associated with critical load protection and cost-optimization that were identified in this study. Also, in comparison with other research studies on MPC based microgrids [11], the results demonstrate improved critical load preservation (up to 32%) and total operational cost reductions (30%) using the proposed method in contrast to the other methods. These results indicate that the proposed method provides more reliable and economical options than previous approaches.

3.5. Comparative analysis of microgrid operational modes

This section presents a comparative analysis of four operational modes in microgrid management, evaluating their performance in terms of operating cost, load reduction, and load prioritization (see Table 6). The study highlights trade-offs between economic efficiency, load management effectiveness, and stability across different control strategies. As seen in the Table 6, a comparative analysis was performed on the operating costs, load distribution among the priority classes, and variability of each of the four operational methods. The results indicated that Method 2 and Method 4 had the same optimum load reduction levels across the secondary and non-critical loads, with zero PV curtailments in all four methods. The results also demonstrate the value of a hierarchical approach to load management. In addition, Method 1 had the lowest total operating cost, but was an effective solution for the reduction of only non-critical loads. Therefore, Method 1 is limited in terms of load distribution. Method 3 had a significantly higher total operating cost than Methods 2 and 4; however, it does provide for improved distribution of non-critical loads at a cost of increase variability compared with the two hierarchical methods. Therefore, the key take-away from this analysis is that both Methods 2 and 4 provide excellent data regarding the efficiency of renewable energy.

Table 6. Comparative performance analysis of four operational modes in microgrid management

Mode	Comprehensive operating cost	Load reduction (kWh)	Abandoned PV rate (%)	Important load removed (kWh)	Secondary load removed (kWh)	Non-critical removed (kWh)	Variance
Mode 1 (No MPC)	100.52	143.82	0.00	0.00	5.55	138.26	0.00
Mode 2 (Load Importance)	257.57	232.45	0.00	0.00	32.97	199.48	0.01
Mode 3 (TOU)	225.97	169.54	0.00	27.41	66.59	75.54	0.02
Mode 4 (Proposed)	257.57	232.45	0.00	0.00	32.97	199.48	0.01

3.6. Forecasting validation and comparative analysis

We quantitatively evaluated the accuracy of the hybrid forecasting framework through statistical assessment of both PV generation forecasts and load demand forecasts. Specifically, each of the four forecasting models utilized was compared to a hybrid ARIMA model plus RF model using a set of common statistical performance metrics, including mean absolute error (MAE) and root mean square error (RMSE). The hybrid ARIMA + RF model was compared to three baseline models (i.e., a standalone ARIMA model, LSTM model, and Prophet model) using data from a year-long dataset consisting of PV generation and load demand forecasts, with a training/validation/test set division of 70/15/15 and the same input feature set. The LSTM model employed a structure with two hidden layers with 64 and 32 neurons, respectively, followed by a fully connected output layer that utilized a linear activation function. The model was trained with a 24-hour input window to gather diurnal trends, an Adam optimizer (with a learning rate of 0.001), a batch size of 32, and 100 epochs, with an early stopping mechanism to reduce overfitting. The prophet model was developed by Facebook and incorporates several features to account for the additive seasonality (daily and weekly) and a piecewise linear trend plus holiday smoothing. Hyperparameters for the Prophet model was determined through cross-validation to minimize the forecast error over the various forecasting horizons (6–24 hours). The results presented in Table 7 demonstrate that the proposed hybrid ARIMA + RF model achieves the lowest prediction errors for both PV and load forecasting tasks, confirming its superior capability to capture nonlinear dependencies and stochastic variations in renewable generation and consumption.

The use of a hybrid model has resulted in a significant decrease in RMSE of around 37% for PV and 32.2% for load forecasting when compared to using ARIMA alone. Furthermore, due to the hybrid model providing more consistent intra-day updates during high generation times; this will lead to improved MPC capabilities while in dynamic operation mode. This continues to improve the ability for an increased level of predictive accuracy towards the scheduling process and priority load statement during the follow-up optimization processes. As opposed to the LSTM and Prophet deep learning models, this hybrid method of

training requires considerably less input training data, less computational time, but still achieves a comparable level of accuracy due to the method combining the best attributes of ARIMA's time-based predictions with the non-linear learning functions provided by RF.

Table 7. Forecasting accuracy comparison for PV generation and load demand

Forecasting model	PV MAE	PV RMSE	Load MAE	Load RMSE	Key features
ARIMA	8.9	11.6	9.4	12.1	Linear time-series baseline
Prophet	8.2	10.5	8.8	11.2	Seasonality + trend decomposition
LSTM	7.4	9.8	7.9	10.4	Deep nonlinear temporal learning
Random forest	6.3	8.4	6.7	8.9	Nonlinear ensemble regression
Proposed Hybrid (ARIMA + RF)	5.6	7.3	6.1	8.2	Combines statistical stability with nonlinear correction

4. CONCLUSION

This study has developed a novel predictive model incorporating a hybrid combination of Forecasting and MPC for the scheduling of islanded microgrids when reliability constraints exist. The load management scheme proposed within this study has achieved significantly greater levels of operational reliability, providing an average 32% increase in the protective capabilities for critical loads, and has not curtailed any PV generation over the period of testing. The developed method combined an optimal arrangement of two types of energy storage systems (both 300 kWh) with a load management scheme which bases priority for using discretionary load resources. This allows the optimization of these two different types of resources so as to achieve a balance between minimizing costs, maximizing the use of renewable energy, and maximizing service reliability. The levels of sensitivity indicate that increasing the capacity of storage systems can lead to around 33.3% reduction in total load shedding and approximately 30% reduction in cost. A comparison between four operation modes has shown that the integrated framework outperforms all other modes with regard to the supply of critical loads while allowing for optimal assignment of time of use pricing to secondary/non-essential loads and optimal intra-day rolling scheduling. Hence, this approach is ideal for areas with high penetration levels of RES and therefore can support more resilient Microgrid deployment. Although validated through high-fidelity simulation, the methodology is based on synthetic data; therefore, validation with actual measurements is the work that will need to be completed for future studies. Implementation of the model predictive control (MPC) algorithm as a part of MATLAB/Simulink will be completed by interfacing it with inverter controllers. Using this approach allows performance evaluation of the MPC controller while considering inverter non-linearities, communication time delays, and measurement noise in an effort to help close the gap between theoretical optimization of control solutions and their use as a control solution in practice for islanded microgrid systems. Future developments may include extending the developed MPC algorithm to cover developing clusters of multiple microgrids cooperating together to share energy and enhance resilience, while incorporating advanced machine learning based forecasting techniques, such as LSTM and gated recurrent units (GRU), into the operational development of the MPC algorithm to support even greater levels of robustness. Stochastic formulations or robust formulations of the MPC controller may be some other ways to effectively manage the uncertainty associated with variable renewable generation and variable energy demand. Future work may also include consideration of electric vehicle (EV) charging as a form of flexible resource, and also the use of blockchain technology for transaction-type processing in order to provide secure, data-based operation of microgrid systems.

ACKNOWLEDGMENTS

The research grants the support of the College of Engineering, Mustansiriyah University (https://webmail.uomustansiriyah.edu.iq).

FUNDING INFORMATION

There is no funding agency that have supported this work.

AUTHOR CONTRIBUTIONS STATEMENT

This journal uses the Contributor Roles Taxonomy (CRediT) to recognize individual author contributions, reduce authorship disputes, and facilitate collaboration.

Name of Author	C	M	So	Va	Fo	I	R	D	O	E	Vi	Su	P	Fu
Dunya Sh. Wais	✓	✓	✓	✓	✓	✓		✓	✓	✓			✓	✓
Huda A. Abbood		✓	✓			✓		✓	✓	✓	✓	✓		✓

C : **C**onceptualization
M : **M**ethodology
So : **So**ftware
Va : **Va**lidation
Fo : **Fo**rmal analysis
I : **I**nvestigation
R : **R**esources
D : **D**ata Curation
O : Writing - **O**riginal Draft
E : Writing - Review & **E**diting
Vi : **Vi**sualization
Su : **Su**pervision
P : **P**roject administration
Fu : **Fu**nding acquisition

CONFLICT OF INTEREST STATEMENT

The authors declare that they have no known competing financial interests or personal relationships that could have appeared to influence the work reported in this paper.

DATA AVAILABILITY

Data will be made available by the corresponding author, [DSW], upon reasonable request.

REFERENCES

[1] J. Hu, Y. Shan, J. M. Guerrero, A. Ioinovici, K. W. Chan, and J. Rodriguez, "Model predictive control of microgrids – An overview," *Renewable and Sustainable Energy Reviews*, vol. 136, p. 110422, Feb. 2021, doi: 10.1016/j.rser.2020.110422.

[2] K. S. Joshal and N. Gupta, "Microgrids with model predictive control: a critical review," *Energies*, vol. 16, no. 13, p. 4851, Jun. 2023, doi: 10.3390/en16134851.

[3] W. Yang, H. Fang, D. Xu, B. Jiang, and P. Shi, "A stochastic model predictive control-based energy management approach for microgrids with electric vehicles," *IEEE Transactions on Transportation Electrification*, vol. 11, no. 1, pp. 3137–3145, Feb. 2025, doi: 10.1109/TTE.2024.3435426.

[4] Z. Wei, P. W. Tien, J. Calautit, J. Darkwa, M. Worall, and R. Boukhanouf, "Investigation of a model predictive control (MPC) strategy for seasonal thermochemical energy storage systems in district heating networks," *Applied Energy*, vol. 376, p. 124164, Dec. 2024, doi: 10.1016/j.apenergy.2024.124164.

[5] K. Nassereddine, M. Turzynski, H. Bielokha, and R. Strzelecki, "Simulation of energy management system using model predictive control in AC/DC microgrid," *Scientific Reports*, vol. 15, no. 1, 2025, doi: 10.1038/s41598-025-89036-7.

[6] D. Arcos–Aviles, A. Salazar, M. Rodriguez, W. Martinez, and F. Guinjoan, "Model predictive control-based energy management system for an isolated electro-thermal microgrid in the Amazon region of Ecuador," *Energy Conversion and Management*, vol. 310, p. 118479, Jun. 2024, doi: 10.1016/j.enconman.2024.118479.

[7] L. Li, S. Fan, L. Dong, R. Huang, Y. Shen, and G. He, "Multi-time scale scheduling framework for multi-energy system considering demand response: A self-approaching optimal approach," *Energy*, vol. 330, p. 136896, Sep. 2025, doi: 10.1016/j.energy.2025.136896.

[8] A. Cordoba-Pacheco and F. Ruiz, "Optimal energy management in multi-microgrids. a scenario-based MPC approach," in *2024 European Control Conference (ECC)*, Jun. 2024, pp. 3709–3714. doi: 10.23919/ECC64448.2024.10590993.

[9] M. Ali, M. A. Abdulgalil, I. Habiballah, and M. Khalid, "Optimal scheduling of isolated microgrids with hybrid renewables and energy storage systems considering demand response," *IEEE Access*, vol. 11, pp. 80266–80273, 2023, doi: 10.1109/ACCESS.2023.3296540.

[10] S. Seyedeh-Barhagh, M. Abapour, B. Mohammadi-Ivatloo, M. Shafie-Khah, and H. Laaksonen, "Optimal scheduling of a microgrid based on renewable resources and demand response program using stochastic and IGDT-based approach," *Journal of Energy Storage*, vol. 86, p. 111306, May 2024, doi: 10.1016/j.est.2024.111306.

[11] S. Su, P. Ma, Q. Xie, J. Liu, X. Zhuan, and L. Shang, "Optimal scheduling of extreme operating conditions in islanded microgrid based on model predictive control," *Electronics*, vol. 14, no. 1, p. 206, Jan. 2025, doi: 10.3390/electronics14010206.

[12] G. Serale, M. Fiorentini, A. Capozzoli, D. Bernardini, and A. Bemporad, "Model predictive control (MPC) for enhancing building and HVAC system energy efficiency: Problem formulation, applications and opportunities," *Energies*, vol. 11, no. 3, p. 631, Mar. 2018, doi: 10.3390/en11030631.

[13] H. Wang, Y. Huang, A. Khajepour, and Q. Song, "Model predictive control-based energy management strategy for a series hybrid electric tracked vehicle," *Applied Energy*, vol. 182, pp. 105–114, Nov. 2016, doi: 10.1016/j.apenergy.2016.08.085.

[14] Y. Liu, H. Shi, L. Guo, T. Xu, B. Zhao, and C. Wang, "Towards long-period operational reliability of independent microgrid: A risk-aware energy scheduling and stochastic optimization method," *Energy*, vol. 254, p. 124291, Sep. 2022, doi: 10.1016/j.energy.2022.124291.

[15] A. Ghasemi-Marzbali, M. Shafiei, and R. Ahmadiahangar, "Day-ahead economical planning of multi-vector energy district considering demand response program," *Applied Energy*, vol. 332, p. 120351, Feb. 2023, doi: 10.1016/j.apenergy.2022.120351.

[16] B. D. K. Reddy, J. S. Naik, S. V. Kumar, S. Kumar, G. Haritha, and M. R. Reddy, "A methodological review on time series forecasting by using ARIMA," Atlantis Press, 2025, pp. 709–719. doi: 10.2991/978-94-6463-662-8_55.

[17] J. Fattah, L. Ezzine, Z. Aman, H. El Moussami, and A. Lachhab, "Forecasting of demand using ARIMA model," *International Journal of Engineering Business Management*, vol. 10, Jan. 2018, doi: 10.1177/1847979018808673.

[18] W. Zhong *et al.*, "Accurate and efficient daily carbon emission forecasting based on improved ARIMA," *Applied Energy*, vol. 376, p. 124232, Dec. 2024, doi: 10.1016/j.apenergy.2024.124232.

[19] H. A. Salman, A. Kalakech, and A. Steiti, "Random forest algorithm overview," *Babylonian Journal of Machine Learning*, vol. 2024, pp. 69–79, Jun. 2024, doi: 10.58496/BJML/2024/007.

[20] A. Khayat, M. Kissaoui, L. Bahatti, A. Raihani, Y. Atifi, and K. Errakkas, "A novel hybrid GRU-XGBoost model for day-ahead photovoltaic generation forecasting in microgrids," *Scientific African*, vol. 29, p. e02884, Sep. 2025, doi: 10.1016/j.sciaf.2025.e02884.
[21] A. Khayat, M. Kissaoui, L. Bahatti, A. Raihani, K. Errakkas, and Y. Atifi, "Efficient day-ahead energy forecasting for microgrids using LSTM optimized by grey wolf algorithm," *e-Prime - Advances in Electrical Engineering, Electronics and Energy*, vol. 13, p. 101054, Sep. 2025, doi: 10.1016/j.prime.2025.101054.
[22] V. I. Kontopoulou, A. D. Panagopoulos, I. Kakkos, and G. K. Matsopoulos, "A review of ARIMA vs. machine learning approaches for time series forecasting in data driven networks," *Future Internet*, vol. 15, no. 8, p. 255, Jul. 2023, doi: 10.3390/fi15080255.
[23] S. Arifin, M. M. Manurung, S. Jonathan, and P. W. Prasetyo, "Trend analysis of the ARIMA Method: A survey of scholarly works," *Recent in Engineering Science and Technology*, vol. 02, no. 03, pp. 1–14, 2024.
[24] X. Wang, C. Zhang, Z. Qiang, W. Xu, and J. Fan, "A new forest growing stock volume estimation model based on adaboost and random forest model," *Forests*, vol. 15, no. 2, p. 260, Jan. 2024, doi: 10.3390/f15020260.
[25] B. V Praveen Kumar, P. Sivalakshmi, S. Muthumarilakshmi, G. Suresh, K. Vijayalakshmi, and C. Srinivasan, "Real-time monitoring of electrical faults in industrial machinery using IoT and random forest regression," in *2024 Second International Conference on Intelligent Cyber Physical Systems and Internet of Things (ICoICI)*, Aug. 2024, pp. 425–430. doi: 10.1109/ICoICI62503.2024.10696655.
[26] G. Fan, C. Peng, X. Wang, P. Wu, Y. Yang, and H. Sun, "Optimal scheduling of integrated energy system considering renewable energy uncertainties based on distributionally robust adaptive MPC," *Renewable Energy*, vol. 226, p. 120457, May 2024, doi: 10.1016/j.renene.2024.120457.
[27] X. Cao, X. Chen, H. Huang, Y. Zhang, and Q. Huang, "Multi-time scale optimal scheduling of a photovoltaic energy storage building system based on model predictive control," *Energy Engineering*, vol. 121, no. 4, pp. 1067–1089, 2024, doi: 10.32604/ee.2023.046783.
[28] E. Liu, S. Gao, X. Chen, J. Li, Y. Sun, and M. Zhang, "Multi-source energy storage day-ahead and intra-day scheduling based on deep reinforcement learning with attention mechanism," *Applied Sciences*, vol. 15, no. 18, p. 10031, Sep. 2025, doi: 10.3390/app151810031.

BIOGRAPHIES OF AUTHORS

Dunya Sh. Wais was born in Baghdad, Iraq, in 1982. She received her B.Sc. degree in Electrical Engineering (Rank 1) from the College of Engineering, Al-Mustansiriyah University, Baghdad, Iraq, in 2005. She received a Master of Science (M.Sc.) in Electrical Engineering Science from Al-Mustansiriyah University, Baghdad, Iraq, in 2021. Her research interests include intelligent optimization, renewable energy, power electronics, power systems, DC-DC converters, AC drive systems, and Arduino applications. She is an assistant lecturer at the Department of Electrical Engineering, College of Engineering, Mustansiriyah University, Baghdad, Iraq. She can be contacted at email: dunya.sh.wais@uomustansiriyah.edu.iq.

Huda A. Abbood was born in Amarah, Iraq, in 1988. She received her B.Sc. degree in Electrical Engineering (Rank 1) from the Electro-Mechanical Engineering Department, University of Technology, Baghdad, Iraq, in 2011. She received a Master of Science (M.Sc.) in Electrical Engineering Science from Wasit University in 2021. Her research interests include antennas, tunable antennas, IoT, energy harvesting antennas, control modelling, and embedded systems. She is an assistant lecturer at the Department of Electrical Engineering, College of Engineering, Mustansiriyah University, Baghdad, Iraq. She can be contacted at email: hudaabdulameer@uomustansiriyah.edu.iq.